View Online / Journal Homepage / Table of Contents for this issue
Dynamic Article Links

PCCP

Cite this: *Phys. Chem. Chem. Phys.*, 2012, **14**, 502–510

www.rsc.org/pccp

PAPER

Overhauser DNP with ^{15}N labelled Frémy's salt at 0.35 Tesla

Maria-Teresa Türke,[a] Giacomo Parigi,[b] Claudio Luchinat[b] and Marina Bennati*[a]

Received 18th July 2011, Accepted 5th October 2011
DOI: 10.1039/c1cp22332a

Published on 09 November 2011 on http://pubs.rsc.org | doi:10.1039/C1CP22332A
Downloaded by Max Planck Institut fuer on 10 April 2012

The effectiveness of dynamic nuclear polarization (DNP) as a tool to enhance the sensitivity of liquid state NMR critically depends on the choice of the optimal polarizer molecule. In this study the performance of ^{15}N labelled Frémy's salt as a polarizing agent in Overhauser DNP is investigated in detail at X-band (0.35 T, 9.7 GHz EPR, 15 MHz ^{1}H NMR) and compared to that of TEMPONE-D,^{15}N employed in previous studies. Both radicals provide similar maximum enhancements of the solvent water protons under similar conditions but a different saturation behaviour. The factors determining the enhancement and effective saturation were measured independently by EPR, ELDOR and NMRD and are shown to fulfil the Overhauser equation. In particular, following the theory of EPR saturation we provide analytical solutions for the dependence of the enhancement on the microwave field strength in terms of saturation transfer between two coupled hyperfine lines undergoing spin exchange. The negative charge of the radical in Frémy's salt solutions can explain the peculiar properties of this polarizing agent and indicates different suitable application areas for the two types of nitroxide radicals.

I Introduction

In recent years, a multitude of studies on dynamic nuclear polarization (DNP) as a tool to enhance the sensitivity of liquid and solid state NMR experiments have underlined the significance of this technique for high-field NMR investigations of biologically relevant samples.[1–3] The underlying principle of DNP, *i.e.* polarization transfer from a higher polarized electron spin system to nuclear spins by pumping electronic transitions,[4] hinges on the choice of the adequate electron spin system—that is the polarizer species introduced into the sample.

In liquid DNP, the enhancement of the NMR signal ε is described as a product of three quantities, which depend on the intrinsic properties of the chosen polarizer/solvent system and the pumping conditions—*i.e.* the coupling factor ξ, the leakage factor f and the effective saturation factor s_{eff} of the EPR transition(s)—with the gyromagnetic ratio of the electron γ_{e} and the nucleus under investigation γ_{I}:[5]

$$\varepsilon = 1 - s_{\mathrm{eff}} f \xi |\gamma_{\mathrm{e}}|/\gamma_{\mathrm{I}} \qquad (1)$$

Over the past years it has been established[6–9] that small nitroxide radicals lead to high coupling efficiency and ^{15}N and ^{2}H labelling of the polarizing agent substantially improves the effective saturation achieved upon pumping one of the EPR transitions. At X-band, we have recently reported signal enhancements of the surrounding bulk water protons close to −180 using 25 mM TEMPONE-D,^{15}N (4-Oxo-TEMPO) with saturation and leakage factors approaching unity.[10]

Concomitantly, Prandolini *et al.*[11,12] reported high enhancement factors using the ^{15}N labelled nitroxide Frémy's salt with an *in situ* liquid-state DNP set up at 9 T (260 GHz EPR, 400 MHz ^{1}H NMR). The high performance of this polarizer was mainly attributed to its narrow EPR line width, which allows for higher s_{eff} levels in the non-saturating regime. Such properties are useful particularly at high microwave frequencies, where elevated microwave power levels P_{mw} are difficult to achieve and introduce unwanted microwave heating effects in the aqueous solution. The maximum extrapolated enhancement was found to coincide for Frémy's salt and TEMPONE at rather large concentrations of 40 to 50 mM, suggesting a similar coupling factor despite the smaller molecular size of Frémy's salt.

In this paper we investigate the performance of ^{15}N labelled Frémy's salt in Overhauser DNP at X-band (0.34 Tesla). At this frequency high microwave B_1 fields ($B_1 \approx P_{\mathrm{mw}}^{1/2}$) are available to achieve maximum saturation and hence record the full power dependence of the DNP enhancement.[13] We measure all other factors in the Overhauser equation independently, *i.e.* s_{eff} of the whole electron spin system by pulse electron double resonance (ELDOR) and the coupling factor ξ from nuclear magnetic relaxation dispersion (NMRD).[14]

In the past, several theoretical models were evoked to quantitatively describe the saturation factor of nitroxide radicals.[7,10,15,16] Here, particular interest will be devoted to the description of the B_1 dependence of the effective saturation factor in the case of Heisenberg spin exchange between the two EPR transitions as encountered for ^{15}N labelled nitroxide radicals. To this end,

[a] *Max Planck Institute for Biophysical Chemistry, Am Faßberg 11, 37077 Göttingen, Germany. E-mail: bennati@mpibpc.mpg.de*
[b] *Magnetic Resonance Center (CERM), University of Florence, via Luigi Sacconi 6, 50019 Sesto Fiorentino, Italy*

This journal is © the Owner Societies 2012

Published on 09 November 2011 on http://pubs.rsc.org | doi:10.1039/C1CP22332A
Downloaded by Max Planck Institut fuer on 10 April 2012

the theory of saturation transfer and double resonance effects in EPR[17,18] will be recapitulated.

The results of our study on ^{15}N labelled Frémy's salt are discussed in a systematic comparison with TEMPONE-D,^{15}N in terms of suitability of the two radicals as polarizing agents in liquid state DNP at different frequencies.

II Theoretical background

Previously,[10] we have reported the maximum effective saturation factor achieved for ^{15}N labelled nitroxides when continuously irradiating one of the two hyperfine transitions as a steady-state solution of the coupled rate equations describing the populations of a four-level-system (*e.g.* S = 1/2, I(^{15}N) = 1/2). It is given by

$$s_{\mathrm{eff}}^{\max} = 1 - 1\Big/\left(2 + \frac{w_{1n}}{w_{1e}} + \frac{\omega_{ex}}{2w_{1e}}\right) \qquad (2)$$

and includes the following relaxation rates in solution:[19]

(1) the electron spin lattice relaxation rate $w_{1e} = 1/(2T_{1e})$,

(2) the nitrogen nuclear spin lattice relaxation rate w_{1n},

(3) the Heisenberg spin exchange rate ω_{ex}.

Eqn (2) was also derived by Hyde *et al.*[19] within the framework of saturation transfer and double resonance effects in EPR.[17,18] This theory provides the power dependence of the intensity for each coupled hyperfine line in the EPR spectrum and is outlined in the following.

In the absence of spin exchange a spin system is described by the Hamiltonian

$$\hbar\mathscr{H}(t) = \hbar\mathscr{H}_0 + \hbar\mathscr{H}_1(t) + \hbar\varepsilon(t) \qquad (3)$$

and contains the time independent Hamiltonian $\mathscr{H}_0$, randomly modulated perturbations of the lattice leading to relaxation effects $\mathscr{H}_1(t)$ and the contribution from the interaction of the electron spins with the microwave field $\varepsilon(t)$. Here the Hamiltonian is presented in units of angular momentum, *i.e.* divided by the reduced Planck constant $\hbar$.

In the high-field approximation for one electron and i coupled nuclei experiencing a static magnetic field B_0 along the z-direction, we can write

$$\hbar\mathscr{H}_0 = g_e\mu_B B_0\hat{S}_z - \hbar\textstyle\sum_i\gamma_i\hat{I}_{zi}B_0 - \hbar\gamma_e\sum_i a_i\hat{S}_z\hat{I}_{zi} \qquad (4)$$

with the well-known terms for electronic Zeeman, nuclear Zeeman and isotropic hyperfine interactions. The electron and nuclear spin operators along z are represented by $\hat{S}_z$ and $\hat{I}_{zi}$ and the averaged values of the g-tensor and the isotropic hyperfine interactions by g_e and a_i, respectively. μ_B is the Bohr magneton.

Freed[18] expanded the equation of motion of the spin density matrix to consider exchange effects:

$$\dot{\sigma} = -i[\mathscr{H}_0 + \varepsilon(t), \sigma] - \Gamma(\sigma - \sigma_0) + \Phi(\sigma - \sigma_0). \qquad (5)$$

Here $\Gamma(\sigma - \sigma_0)$ and $\Phi(\sigma - \sigma_0)$ are matrices containing the respective relaxation and spin exchange effects, σ_0 is the equilibrium spin density matrix.

Eqn (5) is valid in case the hyperfine lines remain separated during saturation, *i.e.*

$$|\gamma_e B_0|, |\gamma_i B_0|, |\gamma_e a_i|, \tau_c^{-1}, \tau_d^{-1} \gg \varepsilon(t), \Gamma(\sigma - \sigma_0), \tau_{ex}^{-1} \qquad (6)$$

where τ_c is the correlation time describing the motion responsible for $\mathscr{H}_1(t)$ relaxation and τ_d is the duration of contact between an exchanging pair whereas τ_{ex} is an effective exchange time.[18]

A general solution of eqn (5) and definitions of the relaxation and spin exchange matrices can be found in ref. 17, 18, and 20.

Here we consider a four level system for coupled spins S = 1/2, I = 1/2 in a static magnetic field as relevant for ^{15}N labelled nitroxides.

Then, considering the deviation of the spin density matrix from thermal equilibrium under the effect of an oscillating field (with angular frequency ω and strength B_1) defined by

$$\chi \equiv \sigma - \sigma_0 \qquad (7)$$

a steady state solution was given with the matrix elements describing the two electronic transitions factorized in the following way:

$$\chi_1{:} = \langle\downarrow\uparrow|\chi|\uparrow\uparrow\rangle = Z_1 e^{i\omega t} \qquad (8a)$$

$$\chi_2{:} = \langle\downarrow\downarrow|\chi|\uparrow\downarrow\rangle = Z_2 e^{i\omega t} \qquad (8b)$$

Z_1 and Z_2 are time-independent steady state solutions describing the effect of continuous irradiation on the EPR transitions.

In general,[21] the power absorbed by the electron spins is

$$P = -M\frac{\mathrm{d}B_1(t)}{\mathrm{d}t} \qquad (9)$$

with M being the macroscopic magnetization expressed in terms of the spin operator $\hat{S}$, so that $M_\pm(t) = M_x(t) \pm iM_y(t)$ results in:

$$M_\pm = \mathfrak{N}\hbar\gamma_e\mathrm{Tr}[\sigma(t)\hat{S}_\pm]. \qquad (10)$$

$\mathfrak{N}$ represents the spin concentration. Consequently, the power absorbed by the hyperfine line is given as

$$P_i = \mathfrak{N}\hbar\omega\gamma_e B_1\hat{S}_{-,i}Z_i'' \qquad (11)$$

and is proportional to the imaginary part of $Z_i = Z_i' + iZ_i''$.

Hence, Z_1'' and Z_2'' derived from the relevant spin density matrix elements subject to eqn (6) can be used to describe the intensities of the two hyperfine lines. In ref. 17, 18, and 20 a detailed derivation is carried out yielding a matrix equation for the coupled saturated Lorentzian lines with a vector $\boldsymbol{Z''}$ containing Z_1'' and Z_2''. The solutions were given by[19]

$$\boldsymbol{Z''} = \boldsymbol{M}^{-1}(-\boldsymbol{R}^{-1})\boldsymbol{Q}, \qquad (12a)$$

$$\boldsymbol{M} = \boldsymbol{1} + (\boldsymbol{R}^{-1}\boldsymbol{K})^2 + (-\boldsymbol{R}^{-1})\boldsymbol{S} \qquad (12b)$$

with the matrices

$$-\boldsymbol{R}^{-1} = \begin{pmatrix} T_{2e} & 0 \\ 0 & T_{2e} \end{pmatrix},\ \boldsymbol{K} = \begin{pmatrix} \Delta\omega_1 & 0 \\ 0 & \Delta\omega_2 \end{pmatrix},$$

$$\boldsymbol{S} = \begin{pmatrix} (1/4)\gamma_e^2 B_{1,1}^2\Omega_1 & (1/4)\gamma_e^2 B_{1,1}B_{1,2}\Omega_{1,2} \\ (1/4)\gamma_e^2 B_{1,1}B_{1,2}\Omega_{2,1} & (1/4)\gamma_e^2 B_{1,2}^2\Omega_2 \end{pmatrix} \qquad (13)$$

describing the transverse electronic relaxation determined by the relaxation time T_{2e}—assumed equal for both spin moieties,

Published on 09 November 2011 on http://pubs.rsc.org | doi:10.1039/C1CP22332A
Downloaded by Max Planck Institut fuer on 10 April 2012

the frequency deviations from the two resonance positions $\Delta\omega_1$ and $\Delta\omega_2$ and the saturation, *i.e.* the B_1 fields applied at transitions 1 and 2 as well as the so-called saturation parameters Ω_i and $\Omega_{i,j}$, respectively. $\boldsymbol{Q}$ is a vector containing the population differences of the two transitions with entries $(\hbar/(2kT))\gamma_e B_{1,i}\omega_e$, where k is the Boltzmann constant and T the temperature. The nuclear Zeeman and hyperfine terms are neglected with respect to the electron Zeeman energy $\hbar\omega_e$, so that $\omega_1 = \omega_2 = \omega_e$.

The 'saturation matrix' $\boldsymbol{S}$ expresses the coupling of the two lines as it contains off-diagonal elements and includes the relaxation rates relevant for the polarization transfer process, w_{1e}, w_{1n}, ω_{ex}. In particular, for an S = 1/2, I = 1/2 spin system the saturation parameters are[19]

$$\Omega_1 = \Omega_2 = \frac{2+c}{w_{1e}(1+c)}, \Omega_{1,2} = \Omega_{2,1} = \frac{c}{w_{1e}(1+c)} \quad (14a)$$

where

$$c = \frac{w_{1n}}{w_{1e}} + \frac{\omega_{ex}}{2w_{1e}} \quad (14b)$$

Then each of the two EPR lines is given by[19]

$$Z_i'' = \frac{(\hbar/(2kT))\gamma_e\omega_e B_{1,i} T_{2e}(1-\xi_i/\Omega_{j,i})}{1+\Delta\omega_i^2 T_{2e}^2 + (1/4)\gamma_e^2 B_{1,i}^2 T_{2e}(\Omega_i - \xi_i)} \quad (15a)$$

$$\xi_i = \frac{(1/4)\gamma_e^2 B_{1,j}^2 T_{2e}\Omega_{i,j}\Omega_{j,i}}{1+\Delta\omega_j^2 T_{2e}^2 + (1/4)\gamma_e^2 B_{1,j}^2 T_{2e}\Omega_j} \quad (15b)$$

that corresponds to the familiar Bloch solution[22] with two additional terms ξ_i arising from polarization transfer between the electronic transitions. Obviously the Bloch solution is recovered for $\omega_{ex} \to 0$ and $w_{1n} \to 0$.

In the situation of Overhauser DNP, when one of the lines is actively pumped but both contribute to the overall polarization, it is crucial to investigate the behaviour of both lines and distinguish between the saturation achieved on the pumped and the other ('detected') transition. In the following we will discuss the effective DNP saturation factor as $s_{eff} = (s_{pump} + s_{det})/2$ with $s_{pump} = 1 - Z_1''/Z_0''$ and $s_{det} = 1 - Z_2''/Z_0''$ and Z_0'' corresponding to the signal in thermal equilibrium.

We let $B_{1,2} \to 0$ since this line is not pumped in our DNP experiment and only used for detection by short pulses in the pulsed ELDOR experiments which should not change the saturation level. Only the dependence on the pump power represented by $B_{1,1} \equiv B_1$ is retained. Additionally, we set $\Delta\omega_1 = \Delta\omega_2 = 0$. Then, according to eqn (15a, b), the saturation levels of the two lines are derived as

$$s_{det}(B_1) = \frac{(1/4)\gamma_e^2 B_1^2 T_{2e}(2w_{1n}+\omega_{ex})}{(1/4)\gamma_e^2 B_1^2 T_{2e}(4w_{1e}+2w_{1n}+\omega_{ex}) + w_{1e}(2(w_{1e}+w_{1n})+\omega_{ex})} \quad (16a)$$

and

$$s_{pump}(B_1) = 1 - \frac{w_{1e}(2(w_{1e}+w_{1n})+\omega_{ex})}{(1/4)\gamma_e^2 B_1^2 T_{2e}(4w_{1e}+2w_{1n}+\omega_{ex}) + w_{1e}(2(w_{1e}+w_{1n})+\omega_{ex})} \quad (16b)$$

and the effective saturation factor in Overhauser DNP with ^{15}N labelled nitroxides results in

$$s_{eff}(B_1) = \frac{(1/4)\gamma_e^2 B_1^2 T_{2e}(2(w_{1e}+w_{1n})+\omega_{ex})}{(1/4)\gamma_e^2 B_1^2 T_{2e}(4w_{1e}+2w_{1n}+\omega_{ex}) + w_{1e}(2(w_{1e}+w_{1n})+\omega_{ex})} \quad (17)$$

For full saturation of the pumped line, *i.e.* $B_1 \to \infty$, we recover eqn (2) as should be expected.

In the past, it has been proposed to plot the Overhauser DNP enhancements as $1/(\varepsilon - 1)$ *versus* $1/P$ or $1/B_1^2$ and linearly extrapolate to infinite power.[23] For a single EPR line obeying the Bloch equations the linear behaviour of $1/s$ in $1/B_1^2$ is immediately evident. For the case of two coupled hyperfine transitions, we inspect $1/s_{eff}$ from eqn (17) and find

$$\frac{1}{s_{eff}} = \frac{2(2w_{1e}+w_{1n})+\omega_{ex}}{2(w_{1e}+w_{1n})+\omega_{ex}} + \frac{2}{T_{1e}T_{2e}\gamma_e^2 B_1^2} \quad (18)$$

which indeed represents a straight line with slope $2/(T_{1e}T_{2e}\gamma_e^2)$ and the intercept corresponds to the maximum achievable saturation $1/s_{eff}^{max}$ described by eqn (2).

Then we can rephrase the Overhauser eqn (1) as a linear dependence on $1/B_1^2$

$$\frac{1}{\varepsilon - 1} = \frac{1}{\varepsilon_{max} - 1} - \frac{2}{\gamma_e^2 T_{1e} T_{2e} f\xi(|\gamma_e|/\gamma_I)} \frac{1}{B_1^2} \quad (19)$$

where $\varepsilon_{max} = 1 - s_{eff}^{max} f\xi|\gamma_e|/\gamma_I$ represents the theoretical maximum enhancement and evaluates the maximum effective saturation factor from the intercept whereas the slope contains the saturation factor of the pumped line as known from the Bloch case.

III Results and discussion

CW-EPR line widths and B_1 dependent DNP enhancements

In Fig. 1 we display CW-EPR spectra of ^{15}N labelled Frémy's salt dissolved at three different concentrations, *i.e.* 5, 10, 25 mM, under non-saturating conditions. The EPR line widths at these concentrations are 0.3, 0.4 and 0.8 G, respectively, which correspond to transverse electronic relaxation times of T_{2e} = 232, 168 and 77 ns. This slower transverse relaxation with respect to TEMPONE[9] let us expect to reach maximum EPR saturation and with it maximum DNP enhancement at a lower incident microwave B_1 field than in previous studies on TEMPONE-D,^{15}N.[10,13]

The achieved DNP enhancement factors on the water ^{1}H are plotted over B_1^2 in Fig. 2 at 5, 10 and 25 mM concentration of the polarizing agent. The data were fitted according to eqn (19) by performing a linear fit of $1/(\varepsilon - 1)$ *versus* $1/B_1^2$ (Fig. 2, inset). The fits were redrawn as ε *versus* B_1^2 and are represented together with the data. As can be observed from Fig. 2 and especially from the linear behaviour displayed in the $1/(\varepsilon - 1)$ plots, the measured enhancements follow the theoretical expectations within error. The maximum attainable enhancements—extrapolated to infinite power—which are read from the intercept of the linear fits are in very good agreement with the maximum

 This journal is © the Owner Societies 2012

Published on 09 November 2011 on http://pubs.rsc.org | doi:10.1039/C1CP22332A
Downloaded by Max Planck Institut fuer on 10 April 2012

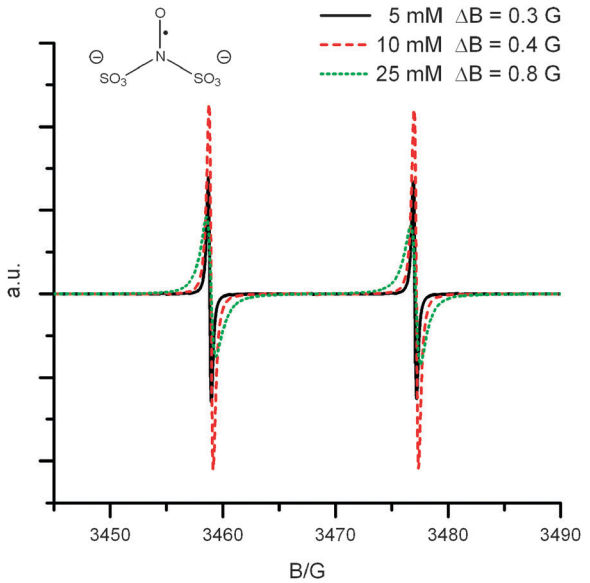

Fig. 1 Continuous wave (CW) EPR spectra at X-band of 5, 10 and 25 mM ^{15}N labelled Frémy's salt. The spectra were acquired at 0.8 mW, modulation amplitude of 0.1 G and time constant of 20 ms. Each spectrum is an average of 4 scans.

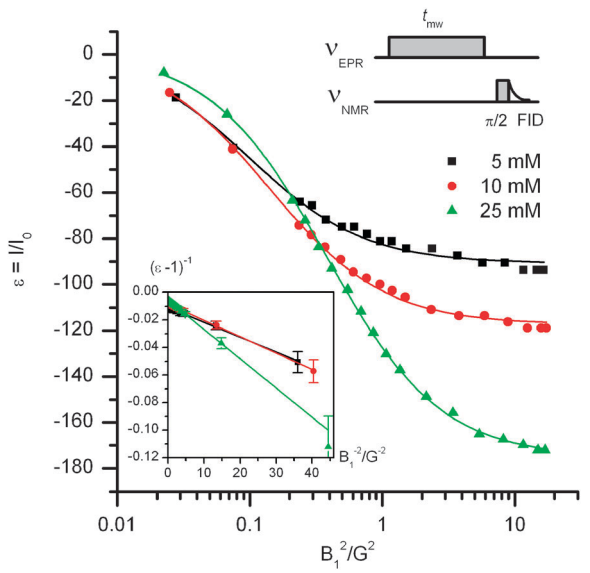

Fig. 2 ^{1}H-NMR signal enhancement of water containing ^{15}N labelled Frémy's salt at 5, 10, 25 mM concentration as a function of the microwave B_1 field. t_{mw} = 4.25, 2.25 and 1 s for these concentrations, respectively. The fits were performed according to eqn (19) of the linear representations (inset) and redrawn for ε *versus* B_1^2.

enhancements actually achieved in the DNP experiment. These values are summarized in Table 1.

Moreover, the B_1 field needed to achieve 90% of the maximum DNP enhancement now lies between ~1 and 2 G—distinctly lower than using TEMPONE-D,^{15}N as polarizing agent, where B_1 values of ~2 to 3 G were needed to reach the same level (see Table 2). This behaviour is consistent with the longer T_{2e} times of Frémy's salt which result in a less steep slope of the $1/(\varepsilon - 1)$ curve according to eqn (19) for similar

Table 1 Overhauser DNP parameters achieved with ^{15}N labelled Frémy's salt as a polarizing agent at room temperature

Conc/ mM	ε (DNP)	ε (fit)	s_{eff} (ELDOR)	s_{eff} (calc)	f (NMRD)	ξ^a
5	−94 ± 13	−91	0.58 ± 0.02	—	0.73	0.34 ± 0.05
10	−119 ± 14	−117	0.67 ± 0.01	0.66	0.83	0.33 ± 0.04
25	−172 ±17	−175	0.86 ± 0.03	0.85	0.92	0.33 ± 0.04

[a] ξ is calculated from the quantities directly measured by DNP, ELDOR and NMRD using eqn (1).

longitudinal relaxation time T_{1e}. The latter will be determined in the context of the polarization recovery experiments.

The highest value of $\varepsilon = -172 \pm 17$ at 25 mM of the present study is comparable to the value derived for 25 mM TEMPONE-D,^{15}N, *i.e.* $\varepsilon = -178 \pm 13$.[10] However, the maximum reached (and also reachable) enhancement factors of the solutions containing ^{15}N labelled Frémy's salt are lower than for TEMPONE-D,^{15}N at 5 and 10 mM polarizer concentration (see Table 2).

As pointed out by Prandolini *et al.*,[11] the observation of similar maximum DNP enhancements at large concentrations also at X-band combined with a different power dependence suggests that the main distinction arises from different saturation behaviour rather than the coupling factor. This is immediately evident from eqn (1) when considering that s_{eff} contains the sole power dependence and should approach unity at high B_1 fields and concentrations as well as $f \to 1$ for $c \to \infty$.[5,7,10]

Evaluation of the saturation and coupling factors

To investigate the factors determining the maximum reachable DNP enhancement within the Overhauser theory as expressed by eqn (1), we have used independent methods, *i.e.* pulsed ELDOR[10] to measure the effective saturation factor s_{eff} and NMRD[14] to deduce the coupling factor ξ.

Fig. 3 illustrates the separate saturation levels of the two coupled hyperfine lines s_1 and s_2 of ^{15}N labelled Frémy's salt at 5, 10 and 25 mM concentration observed in the pulse ELDOR experiment. At the available microwave B_1 field of 2.7 G full saturation is achieved on the irradiated EPR line as visible by the reduction of the EPR FID intensity and therefore maximum effective saturation is achieved like in the DNP experiment at maximum power. The baseline corrected and normalized EPR FID intensity of the high-field EPR line is plotted as a function of the frequency of the saturating ELDOR pulse. The error was estimated by comparison of the saturated FID level to the one observed at an off-resonance field position and is taken into account for the calculation of the overall effective saturation of the two EPR transitions given by $s_{eff} = (s_{pump} + s_{det})/2$. Resulting total saturation levels are 58 ± 2, 67 ± 1 and 86 ± 3% at 5, 10 and 25 mM polarizing agent concentration, respectively. The values at 5 and 10 mM are markedly lower than the ones derived for TEMPONE-D,^{15}N (see Table 2 for comparison) in accordance with lower maximum DNP enhancements at these concentrations.

Table 1 summarizes the effective maximum saturation and maximum enhancement factors obtained with ^{15}N labelled Frémy's salt as polarizing agent. The corresponding leakage factors were derived from the NMR relaxation rates with and

View Online

Table 2 Comparison of ^{15}N labelled Frémy's salt and TEMPONE-D,^{15}N as a polarizer in Overhauser DNP at room temperature

Conc/mM	T_{1e}/ns	T_{2e}/ns	ω_{ex}/MHz	B_1 (90% ε)/G	s_{eff}^{max} (ELDOR)	f (NMRD)	ξ (NMRD)	ε_{max}(DNP)	D (10^{-5} cm^2 s^{-1})	d/Å	τ_D/ps
^{15}N Frémy's salt									2.86–3.05	2.9–3.1	29–31
5	—	232	—	1.0	0.58	0.73	0.34	−94			
10	268	168	3.4	1.2	0.67	0.83	0.34	−119			
25	285	77	16	1.8	0.86	0.92	0.34	−172			
TEMPONE-D,^{15}N[a]									2.87	2.7	26
5	298	86	9.8	1.9	0.78	0.78	0.33/0.35	−131			
10	298[b]	52	20[b]	2.1	0.85	0.88	0.33/0.35	−157			
25	298[b]	25	49[b]	2.7	0.87	0.95	0.33/0.35	−178			

[a] The values were taken from ref. 10, 13, and 14. [b] In this study[10] these parameters were only measured for the 5 mM sample. T_{1e} was assumed equal for all concentrations and ω_{ex} was scaled linearly with concentration.

Published on 09 November 2011 on http://pubs.rsc.org | doi:10.1039/C1CP22332A
Downloaded by Max Planck Institut fuer on 10 April 2012

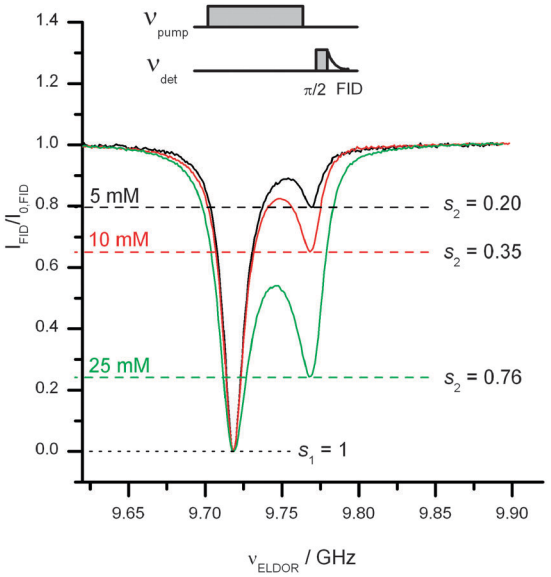

Fig. 3 Normalized and baseline corrected EPR FID intensity of the hyperfine line at 9.74 GHz as a function of the ELDOR frequency, *i.e.* the frequency of the saturating pulse, and of different concentrations of ^{15}N labelled Frémy's salt in aqueous solution at room temperature.

without the polarizing agent at 14 MHz according to eqn (22), Section IV. From these three factors the (concentration independent) coupling factor is determined to be $\xi = 0.33 \pm 0.03$ using the Overhauser eqn (1). This value is indeed identical to the coupling factor of the TEMPONE-D,^{15}N/water system, *i.e.* 0.33 ± 0.02 derived in a similar fashion.[10]

Independently, the coupling factor was determined by NMRD measurements. The water ^{1}H relaxation rate profiles were recorded for 5, 10 and 25 mM concentration of Frémy's salt as well as for the pure buffer solution and the relaxivity was derived for each concentration. For a linear dependence of the paramagnetic relaxation enhancement on the radical content the relaxivity is expected to emerge as independent of concentration. We have observed that the curves at 10 and 25 mM concentration have deviated to some degree from the one at 5 mM, *i.e.* they are reduced by a factor of 10 and 15%, respectively. However, the evaluation of the coupling factor for purely dipolar interaction (eqn (20), Section IV) is not affected by this rescaling since it basically depends on the ratio of two relaxation rates. Bearing this in mind, the coupling factor is determined to be $\xi_{NMRD} = 0.34$, in excellent agreement with the value derived from the Overhauser equation using ELDOR determined effective saturation factors. It also coincides with our former NMRD based analysis for TEMPONE-D,^{15}N/water which yields a coupling factor of 0.33/0.35 (with/without including a contribution from contact interaction in the fit of the relaxation profiles).[14]

In order to check the assumption of purely dipolar interaction for Frémy's salt and to determine the relaxation parameters such as diffusion constants and distance of closest approach, a fit of the proton relaxivity was performed similar to the former study on TEMPONE.

The fit displayed in Fig. 4 was accomplished exclusively using outer-sphere relaxation while the inclusion of inner-sphere contributions decreases the quality of the fit. Similar to solutions containing TEMPONE-D,^{15}N the diffusion coefficient amounts to $D = 2.86 \cdot 10^{-5}$ cm^2 s^{-1}.[14] Remarkably, the distance of closest approach is somewhat larger for Frémy's salt, *i.e.* $d = 2.9$ Å resulting in a larger correlation time of 29 ps (eqn (21), Section IV) despite its smaller molecular size.

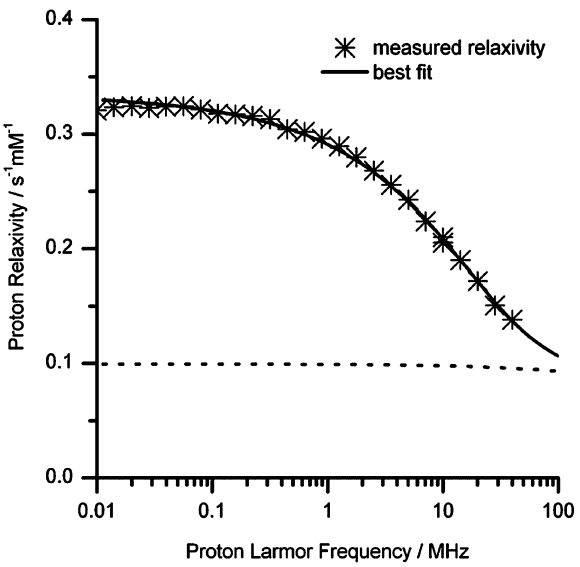

Fig. 4 Proton relaxivity of aqueous solutions containing ^{15}N labelled Frémy's salt depending on the nuclear Larmor frequency as measured in a field cycling relaxometer together with the best fit using outer-sphere contributions and the term resulting solely from nuclear dispersion as dashed line. The relaxation curve of the 5 mM sample was used as basis for this profile.

 This journal is © the Owner Societies 2012

Published on 09 November 2011 on http://pubs.rsc.org | doi:10.1039/C1CP22332A
Downloaded by Max Planck Institut fuer on 10 April 2012

The deviation observed in the relaxivity mentioned above for higher radical concentrations may be caused by an error in the estimation of the radical concentration; indeed we observed that Frémy's salt tends to precipitate at higher concentrations if a variation of the temperature occurs. If the fit is performed using the profile collected with the 25 mM sample, values of $D = 3.05 \cdot 10^{-5}$ cm^2 s^{-1}, $d = 3.1$ Å and $\tau = 31$ ps are found with a slightly increased discrepancy to the parameters of TEMPONE-D,^{15}N (see Table 2 for comparison).

Overall it can be concluded that the differences in the performance of ^{15}N labelled Frémy's salt as a polarizing agent in Overhauser DNP chiefly originate in its specific saturation behaviour.

Polarization recovery studies

Consequently, we have performed a study of the relevant relaxation rates governing polarization transfer to the coupled hyperfine line and thereby determining the effective saturation factor by polarization recovery EPR (PREPR) and (PRELDOR) experiments. The recovery curves of the EPR FID intensity at the high-field position were measured after initial polarization of either the same or the other (coupled) hyperfine line at 5, 10 and 25 mM polarizing agent concentration. The curves—illustrated in Fig. 5—were fitted using a biexponential function with shared time constants previously described.[10,24–26] Since the nitrogen nuclear relaxation rate is negligible with respect to the electronic relaxation rate as evident from the small polarization transfer effect at 5 mM (Fig. 3) it is omitted in the analysis of the relaxation rates. However, this additionally means that Heisenberg spin exchange plays only a minor role at this concentration, too, and we do not use the corresponding recovery curves for the analysis of the relaxation times. In contrast, 5 mM TEMPONE-D,^{15}N has already exhibited pronounced exchange effects.[10] The fits of the recovery curves at 10 and 25 mM ^{15}N labelled Frémy's salt result in $T_{1e} = 268$ and 285 ns as well as $\omega_{ex} = 3.4$ and 16 MHz, respectively. From these values we have calculated the expected effective saturation factors for these two concentrations using eqn (2). The obtained saturation levels are in good agreement with the measured saturation obtained from ELDOR experiments (see Table 1).

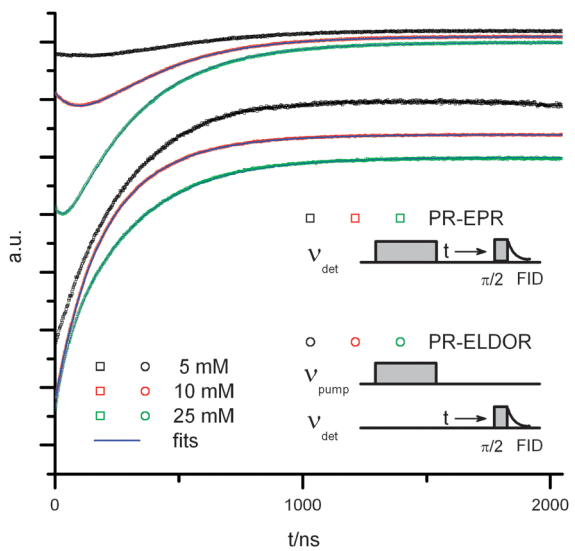

Fig. 5 Recovery curves of the EPR FID in polarization recovery EPR (□) and ELDOR (○) for three concentrations of ^{15}N labelled Frémy's salt. For each of the 10 and 25 mM concentrated samples a biexponential fit with shared time constants was performed on the corresponding PR-EPR and PR-ELDOR trace (—).

In the past, several studies have been performed to examine the concentration dependence of the spin exchange exhibited by Frémy's salt.[27–29] In the earlier studies a non-linear dependence of the exchange rate on concentration C was found by analysing the EPR linewidths which can be expressed by $\omega_{ex} = K(C)C$ and a concentration dependent proportionality factor K. Later Bales and Peric[29] stated that K depends on temperature, viscosity, charge of nitroxide, ionic strength and possibly steric factors, whereas C influences ionic strength and viscosity. They could minimize the dependence of K on C by keeping all of the above mentioned quantities stable and found a linear dependence of ω_{ex} on concentration yielding $\omega_{ex}/C = 9.6 \cdot 10^8$ s^{-1} M^{-1} at 67 °C by EPR line shift and line shape analysis. We note that in our experiments the ionic strength and the viscosity vary with polarizing agent concentration and accordingly the two values of ω_{ex} derived at 10 and 25 mM indicate a non-linear dependence on concentration.

Comparison of Frémy's salt and TEMPONE-D,^{15}N as DNP polarizing agents

In Table 2 the factors of the Overhauser eqn (1) and the relaxation parameters are compared for ^{15}N labelled Frémy's salt and TEMPONE-D,^{15}N. The differences in the maximum enhancement levels can be directly correlated with the differences in the effective maximum saturation factors.

The leakage and coupling factors basically coincide for the two radicals although the molecular size of Frémy's salt is smaller. However, the diffusion coefficient should not be strongly affected by the size since it is mainly determined by the fast motion of the water molecules and indeed it remains almost equal for the two molecules. In contrast, the distance of closest approach is even slightly larger for Frémy's salt and hence also the correlation time. Since the unpaired electron is located at the same subgroup (N–O) in both radicals, these results indicate that the access of water molecules to this group should be somewhat hindered in Frémy's salt. These findings are in agreement with a recent molecular dynamics (MD) and electron-nuclear double resonance (ENDOR) study by Heller *et al.*,[30] in which it was observed that the electron-rich sulfonate oxygens are fully solvated with hydrogen bonds whereas the coordination number of the nitroxide oxygen is reduced. This is attributed to steric hindrance by the sulfonate groups making the nitroxide group difficult to access. In our study this is reflected in the fact that the NMRD relaxation profiles are better fitted without appreciable inner-sphere contributions as opposed to the former study with TEMPONE-D,^{15}N[14] where a slight improvement of the fits was achieved by its inclusion.

The presence of the charged sulfonate groups can also explain the observed differences in the effective maximum saturation factors. For both polarizing agents s_{eff}^{max} given by eqn (2) is mainly determined by the exchange term since T_{1e} is quite similar and the contribution of the nitrogen nuclear relaxation

Published on 09 November 2011 on http://pubs.rsc.org | doi:10.1039/C1CP22332A
Downloaded by Max Planck Institut fuer on 10 April 2012

can mainly be neglected. However, ω_{ex} depends on the nature of bimolecular encounters of the radical molecules. Since Frémy's salt forms radical anions these molecules are repulsive and therefore the distance of closest approach between two radical molecules is increased so that the exchange integral J decreases. This in turn lowers the efficiency of spin exchange which is clearly visible in the overall smaller exchange rates of ^{15}N labelled Frémy's salt with respect to TEMPONE-D,^{15}N resulting in lower maximum saturation levels. Specifically, it was found[28] that Frémy's salt exhibits intermediate exchange instead of the strong exchange observed for most other radicals.

At the same time, transverse relaxation is severely decreased as expressed by the long T_{2e} times displayed by Frémy's salt. This leads to saturation of the pumped EPR transition at rather low B_1, that is, the slope in eqn (18) and (19), which contains the Bloch saturation factor, is steeper than for other polarizing agents such as TEMPONE. The B_1 fields needed to achieve 90% of the maximum enhancements illustrate this fact. At certain B_1 levels below full saturation it is therefore possible that a higher enhancement is achieved with Frémy's salt despite lower maximum enhancements.[11]

Therefore, the main advantage of using ^{15}N labelled Frémy's salt as a polarizing agent for liquid state DNP instead of other nitroxide radicals such as TEMPONE-D,^{15}N is in its easy saturation of the single hyperfine lines. It is particularly useful if the DNP experiment is power limited or heating effects at high microwave power have to be avoided and may therefore play an important role at high microwave frequencies where these issues are especially severe.

In the present X-band study, where full saturation can easily be achieved and heating effects are not an issue, Frémy's salt provides lower enhancements than TEMPONE-D,^{15}N at 5 and 10 mM concentration. Going to higher concentrations such as 25 mM where s_{eff} and f are close to 1 both polarizing agents provide equal enhancements.

IV Materials and methods

^{15}N labelled Frémy's salt

All experiments were carried out using ^{15}N labelled Frémy's salt as paramagnetic species, that is the paramagnetic nitrosodisulfonate anion $ON(SO_3^-)_2$ from $K_2ON(SO_3)_2$, which was synthesized in house. To increase the stability of Frémy's salt it was dissolved in 50 mM K_2CO_3 buffer (pH $\approx$ 11) solution. Samples of 5, 10 and 25 mM concentration of ^{15}N labelled Frémy's salt were prepared. These were degassed for 10 min by N_2 flow, loaded into 0.45 mm inner diameter (ID) tubes and sealed.

The radical concentration was checked by optical absorption[31] and EPR double integral intensities as compared to other nitroxides (TEMPONE, TEMPOL). The EPR signal intensity of Frémy's salt was found to remain stable for several months if stored at 4 °C.

DNP experiments

DNP was performed with the DNP spectrometer at X-band (0.35 T, 9.7 GHz EPR, 15 MHz ^{1}H NMR) described in ref. 13. The microwave B_1 field achieved with this setup ranges up to 4.8 G and the temperature is known to remain stable at room temperature with the sample tube size used (0.45 mm ID, 3 mm filling height).

The microwave irradiation times were optimized to yield maximum DNP enhancement for each concentration, *i.e.* 1, 2.25 and 4.25 s at 5, 10, 25 mM concentration of Frémy's salt. Subsequent to the microwave irradiation the free induction decay (FID) of water ^{1}H was recorded with a 1.5 μs NMR pulse. To calculate the ^{1}H DNP enhancements the first point of the magnitude of the FID was taken as a measure of the intensity I and divided by the corresponding value without preceding microwave irradiation I_0, so that $\varepsilon = I/I_0$. The signal at thermal equilibrium was averaged for 4096 scans and the DNP enhanced signal for 8 scans to complete a full phase cycle. The error of the enhancement was estimated from the noise level of the magnitude FID.

EPR/ELDOR experiments

The continuous wave (CW) EPR measurements as well as the pulsed ELDOR and polarization recovery EPR (PREPR) and ELDOR (PRELDOR) measurements were conducted on a pulsed Bruker ElexSys 580 X-band spectrometer utilizing the same ENDOR cavity (Bruker EN4118X-MD4) as employed for DNP. During the pulsed experiments the cavity was overcoupled and a TWT amplifier was used that can provide B_1 levels up to 10 G in this setup. A 12 ns detection pulse was applied to register the EPR FID which was set 40 MHz off-resonance to the high-field side of the high-field line so that simultaneous detection of both EPR transitions was avoided. In the pulsed ELDOR experiment, a 1 μs saturating pulse was applied in the ELDOR channel prior detection and the ELDOR frequency was swept stepwise over the range of the EPR spectrum.

For the polarization recovery traces the ELDOR pulse was reduced to 100 ns and it excites at a fixed frequency of either the detected (PREPR) or the coupled hyperfine line (PRELDOR) while the time delay to the detection pulse was incremented in steps of 2 ns. All experiments were carried out at room temperature.

NMRD experiments

The NMRD relaxation profiles at 298 K were obtained using a fast field cycling relaxometer[32] that records the ^{1}H relaxation rates in a range of 0.01 to 40 MHz.

After subtraction of the relaxation rates of the buffer and division by the radical concentration, *i.e.* 5, 10, 25 mM, the proton relaxivity in the presence of ^{15}N labelled Frémy's salt was obtained. For a purely dipolar mechanism as can be assumed for nitroxide radicals[33–35] the coupling factor at a nuclear frequency ω_I can be calculated from the observable nuclear relaxation rates R_1

$$\xi = \frac{5}{7}\left(1 - \frac{2w_I}{R_1(\omega_I) - R_1^0}\right). \qquad (20)$$

Here, $2w_I$ corresponds to the relaxation value at very high ω_I (which is 3/10 of the relaxation value at a very low field), R_1 is directly measured at the desired ω_I with the polarizing agent while R_1^0 is the diamagnetic relaxation rate.

 This journal is © the Owner Societies 2012

Published on 09 November 2011 on http://pubs.rsc.org | doi:10.1039/C1CP22332A
Downloaded by Max Planck Institut fuer on 10 April 2012

Furthermore, the curves were fitted according to the full theory for dipolar relaxation as previously discussed,[14] so that the diffusion coefficient D and the distance of closest approach d could be obtained. The correlation time is then defined as

$$\tau_D = \frac{d^2}{D} = \frac{d^2}{D_{water} + D_{radical}} \quad (21)$$

Note that this correlation time is mainly determined by the diffusional coefficient of water D_{water} and the distance of closest approach and is therefore not concurrent with the correlation time τ_c mentioned earlier (eqn (6)) depending on the diffusion coefficient of the radical species, which is picked up in EPR studies.

Additionally, the leakage factors can be derived from the relaxation rates measured with and without polarizing agent

$$f = 1 - \frac{R_1^0}{R_1} \quad (22)$$

They contain the major concentration dependence apart from exchange effects influencing s_{eff}.

V Conclusion

In this study we have investigated ^{15}N labelled Frémy's salt as a polarizing agent in liquid state DNP at X-band (0.35 T, 9.7 GHz EPR, 15 MHz ^{1}H NMR) as compared to TEMPONE-D,^{15}N previously used. The factors of the Overhauser eqn (1) were determined by independent methods such as DNP, NMRD and pulsed ELDOR. They were found to agree with the measured maximum enhancements within error and therefore confirm the validity of this approach for a different polarizing agent.

Here, the dependence of the effective saturation factor on the microwave B_1 field was described within the theory of saturation transfer in EPR.[17,18,20] The maximum achievable effective saturation factor and enhancement depends on the relaxation and exchange rates w_{1e}, w_{1n}, ω_{ex} while the increase with power is described by a 'Bloch-like' factor containing $w_{1e} = 1/(2T_{1e})$ and T_{2e}.

The negatively charged sulfonate groups of Frémy's salt shield the nitroxide group from approaching water molecules, and also repel two approaching polarizing molecules. Therefore, the distance of closest approach of water protons and the associated diffusional time constant are slightly larger than for TEMPONE-D,^{15}N rather than decreasing, as might be expected due to the smaller molecular size. The coupling and leakage factors turn out similar for the two polarizing agents leading to similar maximum enhancements at high concentrations and microwave powers.

Additionally, the distance of closest approach for two Frémy's salt radical anions is also raised so that the exchange rates drop with respect to TEMPONE. This is especially evident at lower radical concentrations where the effective maximum saturation and enhancement factors achieved with ^{15}N labelled Frémy's salt are lower. At the same time less microwave power is necessary to reach maximum saturation caused by slow T_{2e} relaxation.

Hence, ^{15}N labelled Frémy's salt might be an ideal polarizing agent under power-limited conditions as is often the case at high microwave frequencies and corresponding static magnetic fields, *i.e.* in a regime most desirable for high-resolution NMR and biological applications.

Acknowledgements

The work was initially funded by the EU Design Study BIO-DNP and recently by the Max Planck Society. We would like to acknowledge Brigitta Angerstein for her assistance with the synthesis of the Frémy's salt. G.P. and C.L. would like to acknowledge financial support from the BIO-NMR project, contract 261863.

Notes and references

1 M. Bennati, I. Tkach and M.-T. Türke, in *Electron Paramagnetic Resonance*, ed. B. C. Gilbert, D. M. Murphy and V. Chechik, RSC, Cambridge, 2011, 155–182.
2 Special Issue on Dynamic Nuclear Polarization: *Phys. Chem. Chem. Phys.*, 2010, **12**, 5725–5928.
3 Special Issue on Dynamic Nuclear Polarization: *Appl. Magn. Reson.*, 2008, **34**, 213–544.
4 A. W. Overhauser, *Phys. Rev.*, 1953, **92**, 411–415.
5 D. Hausser and D. Stehlik, *Adv. Magn. Reson.*, 1968, **3**, 79–139.
6 D. Grucker, T. Guiberteau, B. Eclancher, J. Chambron, R. Chiarelli, A. Rassat, G. Subra and B. Gallez, *J. Magn. Reson., Ser. B*, 1995, **106**, 101–109.
7 B. D. Armstrong and S. Han, *J. Chem. Phys.*, 2007, **127**, 104508.
8 P. Höfer, G. Parigi, C. Luchinat, P. Carl, G. Guthausen, M. Reese, T. Carlomagno, C. Griesinger and M. Bennati, *J. Am. Chem. Soc.*, 2008, **130**, 3254–3255.
9 P. Höfer, P. Carl, G. Guthausen, T. Prisner, M. Reese, T. Carlomagno, C. Griesinger and M. Bennati, *Appl. Magn. Reson.*, 2008, **34**, 393–398.
10 M.-T. Türke and M. Bennati, *Phys. Chem. Chem. Phys.*, 2011, **13**, 3630–3633.
11 M. J. Prandolini, V. P. Denysenkov, M. Gafurov, B. Endeward and T. F. Prisner, *J. Am. Chem. Soc.*, 2009, **131**, 6090–6092.
12 V. Denysenkov, M. J. Prandolini, M. Gafurov, D. Sezer, B. Endeward and T. F. Prisner, *Phys. Chem. Chem. Phys.*, 2010, **12**, 5786–5790.
13 M.-T. Türke, I. Tkach, M. Reese, P. Höfer and M. Bennati, *Phys. Chem. Chem. Phys.*, 2010, **12**, 5893–5901.
14 M. Bennati, C. Luchinat, G. Parigi and M.-T. Türke, *Phys. Chem. Chem. Phys.*, 2010, **12**, 5902–5910.
15 R. D. Bates and W. S. Drozdoski, *J. Chem. Phys.*, 1977, **67**, 4038–4044.
16 D. Sezer, M. Gafurov, M. J. Prandolini, V. P. Denysenkov and T. F. Prisner, *Phys. Chem. Chem. Phys.*, 2009, **11**, 6638–6653.
17 J. H. Freed, *J. Chem. Phys.*, 1965, **43**, 2312–2332.
18 J. H. Freed, *J. Phys. Chem.*, 1967, **71**, 38–51.
19 J. S. Hyde, J. C. W. Chen and J. H. Freed, *J. Chem. Phys.*, 1968, **48**, 4211–4226.
20 J. H. Freed and G. K. Fraenkel, *J. Chem. Phys.*, 1963, **39**, 326–348.
21 A. Abragam, *Principles of Nuclear Magnetism*, Clarendon, Oxford, 1961.
22 F. Bloch, *Phys. Rev.*, 1946, **70**, 460–474.
23 R. A. Wind and J. H. Ardenkjaer-Larsen, *J. Magn. Reson.*, 1999, **141**, 347–354.
24 J. J. Yin, M. Pasenkiewicz-Gierula and J. S. Hyde, *Proc. Natl. Acad. Sci. U. S. A.*, 1987, **84**, 964–968.
25 B. H. Robinson, D. A. Haas and C. Mailer, *Science*, 1994, **263**, 490–493.
26 W. Froncisz, T. G. Camenisch, J. J. Ratke, J. R. Anderson, W. K. Subczynski, R. A. Strangeway, J. W. Sidabras and J. S. Hyde, *J. Magn. Reson.*, 2008, **193**, 297–304.
27 M. T. Jones, *J. Chem. Phys.*, 1963, **38**, 2892–2895.
28 M. P. Eastman, G. V. Bruno and J. H. Freed, *J. Chem. Phys.*, 1970, **52**, 2511–2522.
29 B. L. Bales and M. Peric, *J. Phys. Chem. B*, 1997, **101**, 8707–8716.

30 J. Heller, H. Elgabarty, B. L. Zhuang, D. Sebastiani and D. Hinderberger, *J. Phys. Chem. B*, 2010, **114**, 7429–7438.
31 J. H. Murib and D. M. Ritter, *J. Am. Chem. Soc.*, 1952, **74**, 3394–3398.
32 G. Ferrante and S. Sykora, *Advances in Inorganic Chemistry–Including Bioinorganic Studies*, 2005, vol. 57, pp. 405–470.
33 W. Müller-Warmuth and K. Meise-Gresch, *Adv. Magn. Reson.*, 1983, **11**, 1–45.
34 C. F. Polnaszek and R. G. Bryant, *J. Chem. Phys.*, 1984, **81**, 4038–4045.
35 D. Sezer, M. J. Prandolini and T. F. Prisner, *Phys. Chem. Chem. Phys.*, 2009, **11**, 6626–6637.

Published on 09 November 2011 on http://pubs.rsc.org | doi:10.1039/C1CP22332A
Downloaded by Max Planck Institut fuer on 10 April 2012

 This journal is © the Owner Societies 2012